catalysts

MDPI

Article

Atoms vs. Ions: Intermediates in Reversible Electrochemical Hydrogen Evolution Reaction

Jurga Juodkazytė [1,*], Kęstutis Juodkazis [1,*] and Saulius Juodkazis [2,3,*]

[1] Center for Physical Sciences and Technology, Saulėtekio Ave. 3, LT-10257 Vilnius, Lithuania
[2] Optical Sciences Center and ARC Training Centre in Surface Engineering for Advanced Materials (SEAM), Faculty of Science, Engineering and Technology, Swinburne University of Technology, Hawthorn, VIC 3122, Australia
[3] World Research Hub Initiative (WRHI), School of Materials and Chemical Technology, Tokyo Institute of Technology, 2-12-1, Ookayama, Meguro-ku, Tokyo 152-8550, Japan
* Correspondence: Jurga.Juodkazyte@ftmc.lt (J.J.); Kestutis.Juodkazis@gmail.com (K.J.); SJuodkazis@swin.edu.au (S.J.)

Abstract: We present a critical analysis of the mechanism of *reversible* hydrogen evolution reaction based on thermodynamics of hydrogen processes considering atomic and ionic species as intermediates. Clear distinction between molecular hydrogen evolution/oxidation (H_2ER and H_2OR) and atomic hydrogen evolution/oxidation (HER and HOR) reactions is made. It is suggested that the main reaction describing *reversible* H_2ER and H_2OR in acidic and basic solutions is: $H_3O^+ + 2e^- \overset{(H_2^+)_{ad}}{\rightleftharpoons} H_2 + OH^-$ and its standard potential is $E^0 = -0.413$ V (vs. standard hydrogen electrode, SHE). We analyse experimentally reported data with models which provide a *quantitative* match (R.J.Kriek et al., Electrochem. Sci. Adv. e2100041 (2021)). Presented analysis implies that *reversible* H_2 evolution is a two-electron transfer process which proceeds via the stage of adsorbed hydrogen molecular ion H_2^+ as intermediate, rather than H_{ad} as postulated in the Volmer-Heyrovsky-Tafel mechanism. We demonstrate that in theory, two slopes of *potential* vs. lg(*current*) plots are feasible in the discussed reversible region of H_2 evolution: $2.3RT/F \approx 60$ mV and $2.3RT/2F \approx 30$ mV, which is corroborated by the results of electrocatalytic hydrogen evolution studies reported in the literature. Upon transition to *irreversible* H_2ER, slowdown of H_2^+ formation in the first electron transfer stage manifests, and the slope increases to $2.3RT/0.5F \approx 120$ mV; R, F, T are the universal gas, Faraday constants and absolute temperature, respectively.

Keywords: H_2ER; H_2OR; HER; HOR; hydrogen; hydrogen molecular ion H_2^+; reversible process

Citation: Juodkazytė, J.; Juodkazis, K.; Juodkazis, S. Atoms vs. Ions: Intermediates in Reversible Electrochemical Hydrogen Evolution Reaction. *Catalysts* **2021**, *11*, 1135. https://doi.org/10.3390/catal11091135

Academic Editors: Vincenzo Baglio and Carlo Santoro

Received: 27 June 2021
Accepted: 16 September 2021
Published: 21 September 2021

1. Introduction

Hydrogen, the most abundant element in the universe, is expected to become carbon neutral fuel of the future. Water, H_2O, is essential to life on Earth and is a source of H_2, which can be generated by water splitting. Production of green hydrogen from water or sea water requires electrolysis using renewable power. This technological step was considered expensive a decade ago [1]. To make it practical, exact mechanisms and reactions with detailed steps and intermediates should be revealed and optimised for the highest efficiency. Electrochemical evolution of hydrogen can take place on the surface of various metals, semiconductor oxides, sulfides as well as other electrically conducting surfaces. Therefore, various issues related with hydrogen evolution reaction are thoroughly analysed in the scientific literature [2–6] with recent search for best performing composites [7,8]. Despite abundant studies in electrochemistry, electro- and photo-catalytic water splitting, there is no quantitatively satisfactory understanding of the hydrogen evolution and oxidation reactions as highlighted recently in [9].

Starting from the first works on this subject [10–12], it was assumed that reduction of H^+ ions proceeds step-wise with formation of hydrogen atoms adsorbed on

the electrode surface, H_{ad}, as intermediates. It is generally accepted that electrochemical hydrogen evolution reaction occurring in acidic aqueous solutions is described by: $2H_3O^+ + 2e^- \overset{H_{ad}}{\rightleftharpoons} H_2 + 2H_2O$, whereas the one proceeding in neutral or alkaline medium is: $2H_2O + 2e^- \overset{H_{ad}}{\rightleftharpoons} H_2 + 2OH^-$. During the cathodic process, adsorbed H_{ad} atoms are removed from the surface via chemical Tafel or electrochemical Heyrovski reactions. Various states such as H_{top}, H_{bridge} and $H_{terminal}$ (according to H-atom position), which differ in their bond strength with the electrode surface are considered [3,13]. Such treatment of hydrogen evolution mechanism is commonly acknowledged and applied for interpretation of various electrocatalytic as well as photoelectrochemical processes taking place on different substrates [14].

The above described mechanism of H_2 evolution process is, however, contradictory, as elaborated further. Firstly, the standard potential of H atom formation is $E^0_{H^+/H} = -2.106$ V [15]. Consequently, the energy of H_{ad} interaction with surface, required to compensate depolarization of H^+ discharge from -2.106 V to 0 V, which is the case for Pt electrode, should be 203.2 kJ mol^{-1}. Such energy is typical to chemisorption, rather than adsorption. Thus, hydrogen atoms are considered to be adsorbed, whereas the indicated values of interaction energy are by far too high for adsorptive interaction. If chemisorption took place, the formation of surface hydrides should occur on the electrode surface, but this is not the case for platinum group metals. In other words, the chemisorption as a prerequisite for the formation of hydrogen atom is replaced by adsorption. Another contradiction is related with the existence of a standard hydrogen electrode (SHE). Recently, in many publications the values of electrochemical potential are reported versus convenient reference hydrogen electrode (RHE) scale [16]. The very existence of such a reference electrode implies that a reversible two-electron transfer process ($2H^+ + 2e^- \rightleftarrows H_2$) with a Nernstian shift of $\frac{dE^0}{d(pH)} = \frac{2.3RT}{F} \approx 60$ mV is feasible on Pt electrode surface under certain conditions (R is the gas constant, 8.135 J K^{-1}mol^{-1}, T is the absolute temperature, taken to be equal to 298 K in the expression above, F is the Faraday's constant, 96,845 C mol^{-1}, and 2.3 is a conversion factor from the natural log to log10). If so, then what is the real mechanism of hydrogen evolution reaction?

This work presents counter arguments for the commonly accepted treatment of hydrogen evolution reaction as well as arguments supporting the alternative concept of this process [17], which provides the *quantitative* explanation of the simultaneous charge and mass changes occurring on Pt electrode under the hydrogen evolution conditions. This revisiting view is mandated by recent experimental study, which can only explain Pt deposition on a carbon electrode via H_2^+ mediation [18]. Theoretical slopes of *potential* vs. lg(*current*) are derived and compared with the reported experimental results for electrocatalytic hydrogen evolution [19–21].

2. Mechanisms of H and H_2 Evolution/Oxidation Reactions

2.1. Thermodynamics of H Atom Formation

The energy of chemical bond in H_2 molecule is ΔH = 453.6 kJ.mol^{-1}, or $\frac{1}{2}D_{H_2} \approx$ 226.8 kJ.mol^{-1} if calculated per one atom [22]. In electrochemistry, usage of ΔG is more appropriate, since $\Delta G = -nFE^0$ and $\Delta G = \Delta H - T\Delta S$, where G, H and S are the thermodynamic functions (Gibbs free energy, Enthalpy and Entropy, respectively), E^0 is the standard potential, T is the absolute temperature and n is the number of electrons transferred in the reaction. From the electrochemical point of view, the standard potential of the so-called Volmer reaction involving the transfer of the first electron:

$$H^+ + e^- \rightleftarrows H, \quad (1)$$

is $E^0_{H^+/H} = -2.106$ V (SHE) [15] (Figure 1). The transfer of the second electron as well as formation of H_2 molecule occurs in Heyrovsky step:

$$H + H^+ + e^- \rightarrow H_2, \quad (2)$$

the standard potential of which is $E^0_{H,H^+/H_2} = 2.106$ V (SHE) [15], i.e., exactly the same number with an opposite sign. Formal summing of the Equations (1) and (2) yields the well-known summary equation:

$$2H^+ + 2e^- \rightleftarrows H_2, \quad (3)$$

with the value of standard potential $E^0_{2H^+/H_2} = 0$ V (SHE). In other words, formation of H_2 molecule fully compensates the electrochemical energy $\Delta G = -nFE^0_{H^+/H} = 406.4$ kJ mol^{-1}, consumed for the formation of 2 moles of H atoms.

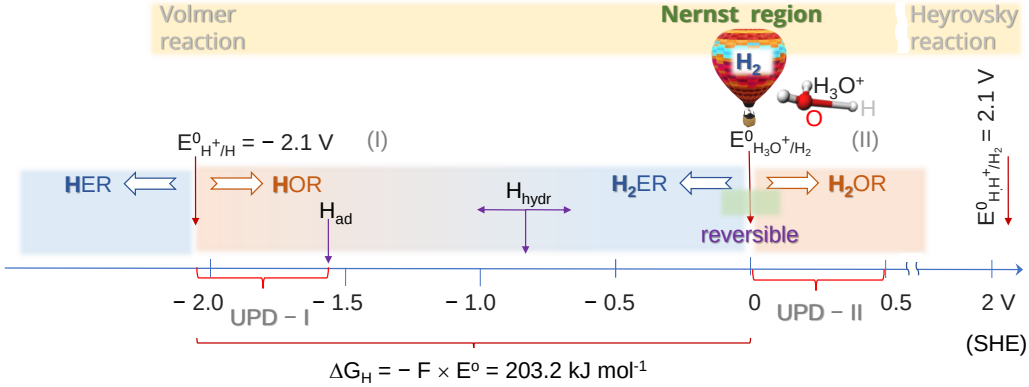

Figure 1. Thermodynamics of atomic (HER/HOR) and molecular hydrogen (H_2ER/H_2OR) processes in the potential range between Volmer and Heyrovsky reactions. The underpotential deposition regions UPD-I and UPD-II correspond to adsorption of H_{ad} and H_3O^+/H_2^+, respectively. The width of regions was evaluated on the basis of 50 kJ mol^{-1}, which is the energy of hydrogen adsorption on Pt reported in the literature [3]. H_{hydr} stands for surface hydrides, formation of which can depolarize the discharge of H^+. The molecular hydrogen evolution and oxidation reactions (H_2ER/H_2OR) are reversible on a Pt electrode in the vicinity of 0 V denoted as Nernst region.

Under standard conditions the actual onset of hydrogen evolution on the surface of platinum group metals is observed at $E = 0$ V (SHE). From the thermodynamic point of view, the transfer of the first electron at $E = 0$ V (SHE) to form H atom should require an adequate energetic compensation. This is logical, since H atoms alone do not exist at normal conditions (room pressure and temperature) due to their highly reactive nature, which is based on an unpaired electron (can be considered a radical) with a short lifetime due to a strong reduction potential. In the context of current study, a hypothetical existence of H atoms could be contemplated if the huge 2.1 eV energy deficit is accounted for (see Figure 1). However, even then, the surface-trapped H-atoms should be immobile due to such chemisorption preventing H_2 formation. Indeed, it is well-known that in case there is a chemical interaction between the electrode surface and the discharging particle, the electrode process becomes depolarized. The effect is called underpotential deposition or UPD, and the extent of depolarization depends on the energy of interaction. In order to depolarize the first electron transfer process from $E^0 = -2.106$ V (SHE) to $E^0 = 0$ V (SHE), the energetic effect of such UPD should be as large as $\Delta G = 203.2$ kJ mol^{-1} (see Figure 1). In the case of anodic hydrogen oxidation reaction on Pt, occurring at even more positive potentials, i.e., within 0–0.5 V (SHE), the energy of interaction between H atom and Pt surface can reach 260 kJ mol^{-1} according to the literature [2,23–26]. Interestingly, the energy of H adsorption on Pt surface evaluated experimentally as well as by recent DFT calculations is reported to range between 9 and 50 kJ mol^{-1} [3,27,28], which is significantly

less than 203.2 kJ mol^{-1} required to justify the existence of H_{ad} on Pt in the vicinity of 0 V (SHE) (see UPD-I region in Figure 1). Thus, there is a profound contradiction between chemisorptive interaction, which could justify the formation of H atom on Pt electrode surface within the discussed E range, and postulated adsorptive interaction deemed to stabilize H_{ad} on the electrode surface.

2.2. Energetics of Bond Breaking in H_2 and H_2^+

The simplest molecular ion H_2^+ attracts interest due to possibility to solve directly quantum mechanical model of its energy structure and to understand formation of covalent bonds [29]. It is useful to compare the above discussed H-atom thermodynamics from a H_2 photo-ionisation point of view. The most efficient generation of H^+ and H (atomic) from H_2 at low pressure takes place via a rovibrational excitation of the H_2(E,F) state, which has one of the strongest known anisotropies of polarisability (5×10^3 times larger than that of H_2 ground state) [30]. There is a large difference of H-H internuclear distance in the ionic inner (E) and covalent outer F-states. By applying an additional strong external laser field of $\sim$ (2–160) TW cm^{-2} intensity at 532 nm wavelength, photo-ionisation and photo-dissociation follows via $H_2^+ \rightarrow H + H^+$ path as revealed by a velocity mapped imaging [30]. Theoretical predictions and experimental verification are closely following each other. An energy cost of this process is formidable considering that H_2(E,F) state is prepared by two-photon absorption at $\lambda = 201.796$ nm wavelengths (photon energy $\hbar\omega = 1.24/\lambda[\mu m] = 6.144$ eV) and an additional two-photon process at $\lambda = 532$ nm (2.33 eV) takes place for transition into the H_2^+ ionised state before photo-dissociation. This is the least energy, hence, a high efficiency pathway of H and H^+ production from H_2. The portion of that energy required for H and H^+ production from H_2^+ is equal to the one photon absorption at green 2.33 eV (similar to $E^0_{H^+/H} = -2.1$ V or -2.31 V [31]; see Figure 1). Equivalence of a potential applied electrically and optically by photon absorption manifests the energy conservation and thermodynamics underpinnings of energy transitions in molecular and ionic species of hydrogen.

The energy difference of molecular bond in H_2 and H_2^+ is $4.48 - 2.69 = 1.79$ eV while the bond length increases from 74 pm (H_2) to 134 pm (H_2^+) [32]. Separation between H-atoms in H_3O^+ is 154.5 pm considering an angle of 107° between hydrogens and the O–H bond length of 96.1 pm. The O–H length can increase by 10 pm during proton transport via the Grotthuss mechanism, and it is 100.5 pm in anion OH^-. It was demonstrated that in addition to a photo-induced dissociation of H_2^+ from the excited vibrational states (stretched molecular ion), a Coulomb explosion also occurs, leading to generation of energetic ($H^+ + H^+ + e$) at laser intensities of $5 \times 10^{13} - 10^{15}$ W cm^{-2} [33]. Bond breaking of H_2^+ defined as a time required to localise an electron onto one of the atoms was directly measured by pump-probe method and found to be 15 fs [34], consistent with theoretical predictions [35].

2.3. Depolarization of H_2 Evolution Due to Hydrogen Molecular Ion H_2^+ Formation

First of all, it should be admitted that depolarization of the electrochemical process can be conditioned by any kind of interaction of the discharging particle with ions or atoms present in its close proximity. In aqueous solutions, there are two particles which can directly take part in H_2 evolution process, i.e., H_2O molecule and H_3O^+ ion. We hypothesize that the main particle irrespective of solution pH is hydronium ion H_3O^+. In neutral and alkaline solutions, a hydronium ion can be produced by dissociation of water molecules according to reaction:

$$2H_2O \rightleftarrows H_3O^+ + OH^- \quad (4)$$

Reaction (4) is fast, because the energy of H–OH bond disruption is compensated by the energy of hydration of H^+ ions, which is as high as 432 kJ mol^{-1} [36]. According to the literature [3], the activation energy of reaction (4) is about 75 kJ mol^{-1}, which is not much; however, the necessity of step (4) to produce hydronium ion in solutions with

pH > 7 can explain why kinetics of hydrogen evolution reaction in alkaline medium is more sluggish [3].

As shown in our previous studies [17,37], the transfer of the first electron during electrochemical discharge of H_3O^+ ion should lead to formation of molecular hydrogen ion H_2^+, whereas the transfer of second electron should yield a H_2 molecule. An important property of H_2^+ ion is the energy of H– H^+ bond, which according to the literature [38] is ΔH^0_{298} = 255.7 kJ mol^{-1}. The energy for the formation of this bond is most likely derived from the energy of hydration of H^+ ion (432 kJ mol^{-1} [36]), which is enough to depolarize the discharge of H^+ from $E^0 = -2.106$ V (SHE) to $E > 0$ V (SHE). The processes occurring at $E = 0$ V (SHE) can be described by the following sequence of electrochemical reactions:

$$H_3O^+ + e^- \rightleftarrows (H_2^+)_{ad} + OH^- \quad (5)$$

$$(H_2^+)_{ad} + e^- \rightleftarrows H_2. \quad (6)$$

Overall reaction is:

$$H_3O^+ + 2e^- \rightleftarrows H_2 + OH^-. \quad (7)$$

In the vicinity of equilibrium potential both processes (5) and (6) are fast and reversible and proceed simultaneously; therefore, the overall two-electron process (7) describes redox processes occurring within certain rate limits on Pt surface in reversible hydrogen electrode (RHE) and determines the magnitude of exchange current, i_0, as well as E of the process. At the equilibrium potential, the exchange current i_0 is equal to the anodic and cathodic components, which are compensating each other, and the total current through the electrode is zero (see Figure 2 and Section 2.4).

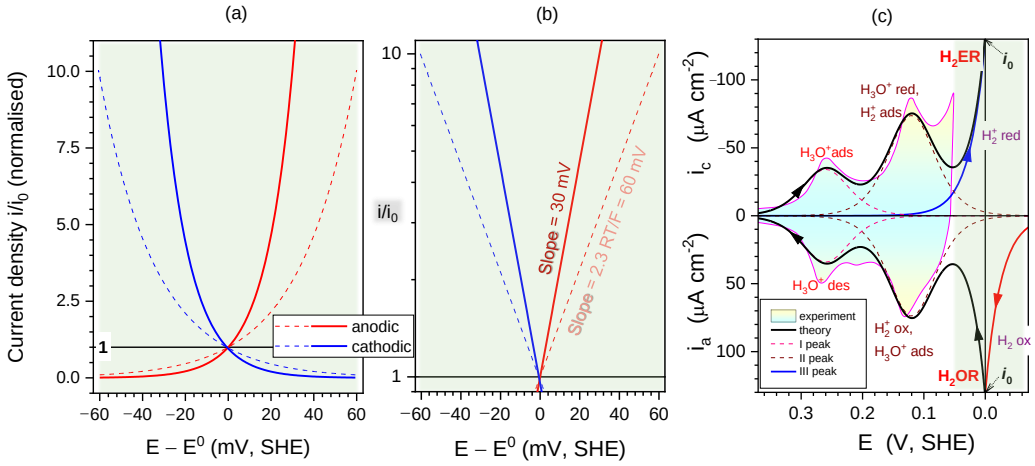

Figure 2. Analysis based on the Nernst equation for reaction (7). (**a**) The reversible polarization curves on Pt modelled for one- (dashed trace) and two-electron (solid trace) transfer processes according to Equation (20). (**b**) The log-line presentation of the same graph (**a**) to reveal the linear slope; i_0 is the exchange current. In experiments [19–21], the slope of 30 mV/dec was determined (solid lines). (**c**) Surface processes leading to H_2ER at 0 V. The proposed model is *quantitatively* matching the experiment of charge and mass changes on the electrode as shown by modelling based on the Nernst equation (adopted from [37]): adsorption and red/ox reactions of ions H_3O^+ and H_2^+ on Pt. The potential locations of the adsorbed (ads), desorbed (des), reduced (red) and oxidised (ox) species are shown by the corresponding markers.

Anodic oxidation of H_2 (H_2OR) proceeds according to reaction (6) and leads to formation of $(H_2^+)_{ad}$ rather than *via* the dissociation to H_{ad} atoms. If reaction (4) is taken into

account, the sum of the Equations (4) and (7) yields the summary equation of reversible hydrogen evolution process:

$$2H_2O + 2e^- \overset{(H_2^+)_{ad}}{\rightleftharpoons} H_2 + 2OH^-. \quad (8)$$

Thus, molecular hydrogen ion $(H_2^+)_{ad}$ should be considered as intermediate in hydrogen evolution process instead of H_{ad} atom. As depicted in Figure 1, H_3O^+ ion accommodates two H^+ ions, which upon addition of two electrons can be used for the formation of H_2 molecule. It is noteworthy that no additional chemical energy except for that resulting from the bond formation between H atoms, is required for Equations (5) and (6). On the contrary, the postulation of the bond between H_{ad} and the surface of platinum group metal acknowledges the need for additional interaction, which inevitably should have an adverse effect on the kinetics of H_2 molecule formation and its detachment from the electrode surface.

Since the existence of reversible hydrogen electrode is an experimentally established fact, the E range above $E^0_{2H^+/H_2} = 0$ V (SHE), known as hydrogen UPD region in the literature and denoted as UPD-II in Figure 1, should, in fact, be related with anodic oxidation of H_2, rather than reduction of H^+ ion to H_{ad} atom. In our previous study [37] on the basis of precise analysis of microgravimetric and coulombmetric data reported in [39], it was demonstrated that the current peaks observed in the voltammograms of Pt electrode in 0.5 M H_2SO_4 within the E range between 0 V and 0.5 V (SHE) are related with reversible adsorption/desorption of the products of anodic oxidation of H_2 molecule, i.e., $(H_3O^+)_{ad}$ and $(H_2^+)_{ad}$ (see Figure 2c for a detailed account of processes). The energy of adsorptive interaction of these surface compounds with electrode surface was evaluated to be 25.1 kJ mol^{-1} and 11.6 kJ mol^{-1}, respectively. In fact, formation of H_{ad} as intermediate in the reduction of H^+ could be hypothesized only in the cathodic range *vs* $E^0_{2H^+/H_2} = 0$ V (SHE), i.e., at $E < 0$ V. It is noteworthy that the formation of surface hydrides (denoted as H_{hydr} in Figure 1) can also depolarize the discharge of hydrogen ions (for details, see Appendix A in ref. [40]).

As one can see from the above discussion, in the case of *reversible* H_2 evolution process (denoted as H_2ER and H_2OR in Figure 1), only those H_2O molecules which are contained in H_3O^+ ion can participate in electrochemical reduction reaction. Other H_2O molecules participate in chemical processes of neutralization or dissociation (Equation (4)). This, however, does not imply that they cannot be electrochemically reduced on the surface under an adequate overvoltage via formation of hydrides, or be reduced chemically to H_2 via the reactions with various electrochemically-produced metal oxide or sulfide surface species. These processes should be analysed, taking into consideration specific conditions of their occurrence, which are outside the scope of the present paper.

2.4. Kinetics and pH-Dependence of E in the Case of Reversible H_2 Evolution/Oxidation Processes

In modern handbooks, one can find two hydrogen evolution equations for aqueous solutions:

$$2H_3O^+ + 2e^- \rightleftarrows H_2 + 2H_2O \quad (9)$$

with $E^0 = 0$ V (SHE) for acidic medium and

$$2H_2O + 2e^- \rightleftarrows H_2 + 2OH^- \quad (10)$$

with $E^0 = -0.826$ V (SHE) for alkaline medium. Both the above reactions are composite and can be subdivided into the steps as follows. For the acidic conditions:

$$H_3O^+ + 2e^- \rightleftarrows H_2 + OH^-,$$

$$OH^- + H_3O^+ \rightleftarrows 2H_2O$$

and for the alkaline conditions:

$$2H_2O \rightleftarrows OH^- + H_3O^+,$$

$$H_3O^+ + 2e^- \rightleftarrows H_2 + OH^-.$$

Thus, the Equation (7) is the same for all media, because the process is the same irrespective of solution pH. The processes of water dissociation (Equation (11)) either precede or follow the electrochemical act (Equation (7)), thus, in fact, there is one ion H_3O^+ or OH^- participating in the two-electron transfer process.

The Nernst equation for reaction (7) is as follows:

$$E = E^0 + \frac{RT}{2F} \times \ln\left(\frac{c_{H_3O^+}}{p_{H_2} c_{OH^-}}\right), \tag{11}$$

where E^0 is the standard potential, R is the gas constant, T is the absolute temperature, $c_{H_3O^+}$ and c_{OH^-} are the concentrations of respective ions and p_{H_2} is the pressure of hydrogen gas. Under standard conditions (p_{H_2} = 1 atm and T = 298 K), $E^0 = -0.413$ V (SHE) in neutral medium where $c_{H_3O^+} = c_{OH^-} = 10^{-7}$ mol l^{-1}, whereas in acidic or alkaline solutions, i.e., at $c_{H_3O^+} = 1$ mol l^{-1} or $c_{OH^-} = 1$ mol l^{-1}, the standard potentials will be 0 V and -0.826 V (SHE), respectively. If $\left[c_{H_3O^+} \times c_{OH^-}\right] = K_w = 10^{-14}$ (where K_w is the ionic product of water), then Equation (11) can be written as:

$$E - E^0 = \frac{RT}{F} \ln c_{H_3O^+} = -2.3\frac{RT}{F} \times pH \tag{12}$$

or

$$c_{H_3O^+} = \exp\left(\frac{F(E - E^0)}{RT}\right) \tag{13}$$

and the time derivative is

$$\frac{dc_{H_3O^+}}{dt} = \exp\left(\frac{F(E - E^0)}{RT}\right) \times \frac{F}{RT}\frac{dE}{dt}, \tag{14}$$

because $(e^x)' = e^x$ and $1/\lg(e) \equiv \ln(10) = 2.303$. On the other hand, it is known that the relation between the rate of electrochemical reaction, i.e., the current i, and the concentration of electroactive species, c, is given by:

$$i = nF \times \frac{dc}{dt}, \tag{15}$$

where n is the number of electrons transferred per one mole and

$$\lg i = \lg(nF) + \lg\left(\frac{dc}{dt}\right) \tag{16}$$

Combination of Equations (16) and (14) yields:

$$\lg i = \lg(nF) + \frac{F(E - E^0)}{RT} \lg e + \lg\left(\frac{F}{RT}\right) + \lg\left(\frac{dE}{dt}\right) = Const + \frac{F(E - E^0)}{2.3RT}, \tag{17}$$

where the cumulative constant $Const = \lg(nF) + \lg\left(\frac{F}{RT}\right) + \lg\left(\frac{dE}{dt}\right)$; the last term is the logarithm of potential sweep rate, which is a constant in electrochemical experiments. From Equation (17) it follows that under standard conditions:

$$d\lg i = \frac{FdE}{2.3RT}, \text{ or } \frac{dE}{d\lg i} = \frac{2.3RT}{F} \approx 60 \text{ mV/dec}. \tag{18}$$

Combination of Equations (14) and (15) yields the expression for reversible polarization curves:

$$i = nF \exp \frac{F(E - E^0)}{RT} \times \frac{F}{RT}\frac{dE}{dt}, \text{ with } i_0|_{E=E_0} = nF \times \frac{F}{RT}\frac{dE}{dt} \quad (19)$$

or

$$i = i_0 \exp \frac{F(E - E^0)}{RT}. \quad (20)$$

These polarization curves for the anodic and cathodic processes are shown in Figure 2a,b, whereas Figure 2c depicts polarization curves of surface electrochemical processes, taking place on the Pt electrode surface in the so-called hydrogen UPD region at $E > 0$ V (SHE). Thus, in the case of *reversible* hydrogen evolution process, the slope $\frac{dE}{d\lg(c)} = \frac{2.3RT}{F}$ is equal to the slope $\frac{dE}{d\lg(i)}$; therefore, it is referred to as the Nernst slope in this study.

Equality $\left[c_{H_3O^+} \times c_{OH^-}\right] = K_w = 10^{-14}$ means that OH^- ion formed in reaction (11) will react with H_3O^+, yielding $2\,H_2O$ and vice versa in the anodic reaction. Consequently, in the case of reversible process, in accordance with Equation (9), where the formal ratio of H_3O^+ to electron is 1:1, the Nernst slope of $\frac{dE}{d\lg(i)} = \frac{2.3RT}{F} \approx 60$ mV/dec and $\frac{dE}{dpH} \approx 60$ mV/pH should be observed. However, if due to some reason the concentration (or activity) of OH^- ions is not decreasing as a result of their interaction with H_3O^+ (e.g., OH^- adsorption on the electrode surface, formation of (hydr)oxides ($MeOH \rightleftarrows Me^+ + OH^-$) or due to some hindrance of their transport at rough nanostructured surfaces), the rate of anodic half-reaction (7) as well as i_0 will increase and the path (7) will become dominant. The Nernst equation for reaction (11), when c_{OH^-} = const and p_{H_2} = 1 atm, can be written as:

$$E = E^0 + \frac{RT}{2F} \times \ln\left(\frac{c_{H_3O^+}}{p_{H_2}c_{OH^-}}\right) = const + \frac{2.3RT}{2F}\lg c_{H_3O^+} = const - \frac{2.3RT}{2F}pH \quad (21)$$

Consequently:

$$\frac{dE}{dpH} = -\frac{2.3RT}{2F} \approx 30\ \text{mV/pH unit} \quad (22)$$

It can also be shown that $\frac{dE}{d\lg i} = \frac{2.3RT}{2F} \approx 30$ mV/dec (detailed derivation of kinetic equations for the case when c_{OH^-} = const is presented in Appendix A).

The E limits, where hydrogen evolution and oxidation reactions proceed reversibly approximately are $\pm\frac{2.3RT}{nF}$, whereas i should not exceed $10 \times i_0$ (Figure 2a,b). When cathodic current significantly exceeds the magnitude of exchange current of reaction (7), i.e., when $i \gg i_0$, transition to irreversible H_2 evolution occurs. In such a case, the transfer of the first electron (Equation (5)) becomes hindered and turns out to be the rate determining step, whereas the transfer of the second electron proceeds instantaneously. The slope $\frac{dE}{d\lg i}$ increases up to $\frac{2.3RT}{\alpha F} = 120$ mV, given that charge transfer coefficient $\alpha = 0.5$, and is referred to as the Tafel slope. Thus, it can be inferred that in the case of hydrogen evolution on Pt electrode, the decrease of slope $\frac{dE}{d\lg i}$ to attain values $\frac{2.3RT}{F} \approx 60$ mV and $\frac{2.3RT}{2F} \approx 30$ mV as the potential approaches the equilibrium potential $E = 0$ V (SHE) demonstrates the transition towards conditions where the process proceeds reversibly.

2.5. Reversibility: Thermodynamics at Work for SHE Electrode

Reversibility is discussed next since the presented H_2ER/H_2OR processes are based on the reversible mechanism (Figure 3). Reversibility is key for thermodynamic analysis and it is essential for existence of the SHE and RHE electrodes. In contrary to full reversibility, the Tafel rate equation defines kinetics of reaction dependent on overpotential, i.e., it is irreversible and non-equilibrium. The Tafel's analysis of I-V characteristic's slope from overpotential $\propto \lg i$ [41] has become a corner stone for analysis of efficiency of electrochemical processes. The phenomenological Butler-[42] and Volmer-[43] model of electrode kinetics fits the Tafel's current-voltage analysis and describes interface pro-

cesses in a microscopic per particle manner. Cases of non-equilibrium thermodynamics encountered at interfaces of fuel cells and batteries, e.g., intercalation, are actively investigated and their reversibility has paramount practical importance [44]. Kinetics of charge transfer on an electrode surface is inherently related to the hydrodynamics of reacting species. It is experimentally established that H_3O^+ diffuses twice faster than OH^- in water, which was explained by ab initio calculations [45] as due to the Grotthuss mechanism dominating over hydrodynamics. Different 3D arrangement of possible proton docking sites is responsible to different probabilities of O–H bond switching. The slower diffusion of OH^- at nanostructured electrocatalytic surfaces is consistent with $\frac{dE}{d\lg i} \approx 30$ mV/dec slope observed experimentally for hydrogen evolution reaction. Other processes such as oxidation/reduction of the electrode, adsorption, chemical reactions and hydrodynamics all can have a contribution to kinetics of H_2ER/H_2OR, especially in the non-reversible region of potentials (Figure 3).

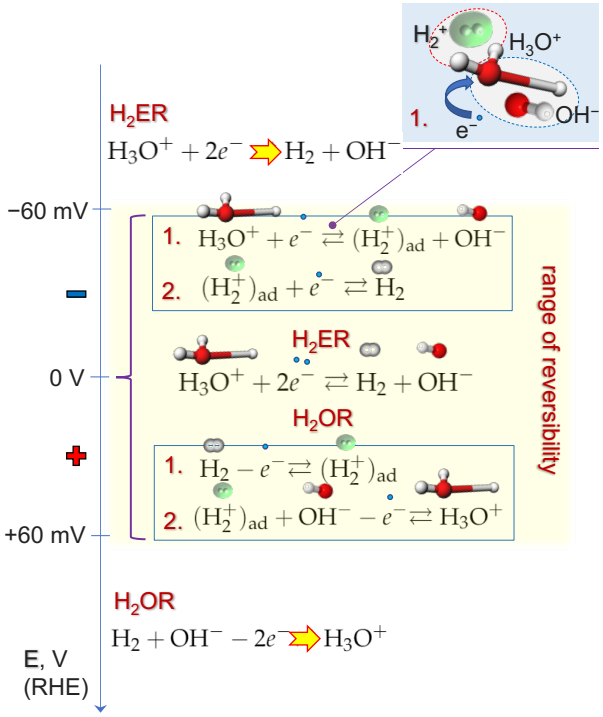

Figure 3. Hydrogen evolution/oxidation reactions H_2ER/H_2OR in aqueous solutions; ⇄ marks reversible processes while the colored arrows in elctrochemical reactions occurring outside the reversibility range of ±60 mV mark irreversible processes. E = 0 V vs. RHE corresponds to equilibrium potential of H_2ER/H_2OR for a solution with any pH. The inset shows schematics of H_2^+ formation (Equation (5)) using pictorials of chemical structures of the participating species. Addition of expressions (1) and (2) in either the positive or negative side leads to the central equation, which defines the equilibrium condition of the SHE (RHE) electrode.

The existence of reversible H_3O^+/H_2, OH^- electrode in the form of SHE or RHE implies the feasibility of a symmetric reversible two-electron transfer process, which proceeds at the same rate in both directions at its equilibrium potential. There is no distinction between those two electrons, as they are transferred simultaneously and the only possible intermediate is the H_2^+ ion. The reversibility of the commonly accepted two-electron process (Equation (3)), which proceeds in a step-wise manner and asymmetrically with $H^+ + e = H_{ad}$ as a forward reaction and $H_2 = 2H_{ad}$ as a backward first step, is questionable. Considering different energetics of the steps, it is highly improbable to have the very same rates as required for the known SHE and/or RHE performance. The hindrance of H_2^+ formation leads to the irreversible hydrogen evolution with Tafel slope of

120 mV/dec found for Pt electrodes [4]. In summary, the essential difference between the conventional HER/HOR and presented here H_2ER/H_2OR hydrogen evolution mechanisms is that H_{ad} is an intermediate stage in the two one-electron transfer steps, whereas H_2^+ is the intermediate in one two-electron transfer reaction. We propose in this thermodynamics-based study that H_2 formation on Pt electrode surface is proceeding via a structural reorganisation inside the H_3O^+ ion, where two neighbouring H-atoms form a bond (they are already at the bond separation) as schematically illustrated in the top-inset in Figure 3. The energy costly and asymmetric process of hydrogen evolution/oxidation via H-atoms contradicts the reversibility of SHE and RHE electrodes, which apparently exists in reality and is used in practice.

3. Conclusions and Outlook

We propose that *reversible* electrochemical hydrogen evolution (H_2ER) occurring in acidic, neutral and alkaline aqueous solutions can be described by one common reaction: $H_3O^+ + 2e^- \overset{(H_2^+)_{ad}}{\rightleftharpoons} H_2 + OH^-$, the potential of which is given by the Nernst equation: $E = E^0 + \frac{2.3RT}{2F} \times \lg\left(\frac{c_{H_3O^+}}{c_{OH^-}}\right)$, where $E^0 = -0.413$ V. The peculiar features of this reaction are as follows: (i) it involves transfer of two electrons per one H_3O^+ and one OH^- ion, (ii) the precursor of H_2 molecule is molecular hydrogen ion $(H_2^+)_{ad}$, which forms during the transfer of the first electron already, whereas the transfer of second electron yields H_2, (iii) the energy of hydration which is conserved within H_3O^+ ion is consumed for the formation of bond in H_2 molecule and accounts for depolarization of H^+ discharge from $E^0_{H^+/H} = -2.106$ V (SHE) to $E > 0$ V, known as hydrogen UPD phenomenon observed on Pt. Based on these considerations, formation of H_{ad} as intermediate in hydrogen evolution/oxidation reactions turns to be thermodynamically and kinetically unfavourable path. It is shown that in the vicinity of reversible potential of hydrogen evolution/oxidation reactions ($E \approx E^0 \pm \frac{2.3RT}{nF}$), two values of $\frac{dE}{dlgi}$ slope are feasible: $\frac{2.3RT}{F} \approx 60$ mV/dec, when $\left[c_{H_3O^+} \times c_{OH^-}\right] = K_w$, and $\frac{2.3RT}{2F} \approx 30$ mV/dec, when $c_{OH^-} = const$. The slope values of ≈ 30 mV/dec found experimentally in the case of electrocatalytic hydrogen evolution process [4,19–21,46] serve as a proof of the alternative mechanism described herein. The twice faster diffusion of H_3O^+ compared to OH^- in water [45] is consistent with the presented model of H_2ER/H_2OR and the experimentally observed 30 mV/dec slope. Presented analysis is further supported by recent experimental results of Pt electrodeposition [18] which are explained by the mechanism involving formation of H_2^+ as intermediate in reversible hydrogen evolution on Pt.

Further insights into energetics and kinetics of H_2ER via H_2^+ intermediate could be provided by the readily available toolbox of density functional theory (DFT) approaches equipped with bond formation modeling at the atomic scale [47], which currently models H atoms instead of H_2^+ [48,49]. Numerical modelling is expected to reveal effects related to non-ideality and surface coverage of active hydrogen species (atoms, ions, molecules), which would expand on the presented ideal case of H_2ER on Pt (also Pd). The theory and modelling should lead to development of practical water splitting applications. In addition to the surface reactions discussed in this study, the same H_2^+ deposition inside solid state of Pd explains the operation principle of optical hydrogen sensor based on metamaterials [50]. Better understanding of the roles of hydrogen atoms, ions (protons) and molecular ions in water splitting and hydrogen sensing will expedite development of future technologies for green power, fuel cells and transportation.

Author Contributions: Conceptualization, K.J. and J.J.; writing original draft, J.J.; visualization, S.J.; discussion and data analysis J.J., K.J., S.J.; all authors contributed to the final editing of the manuscript. All authors have read and agreed to the published version of the manuscript.

Funding: This research received no external funding.

Data Availability Statement: All the data are explicitly provided in the paper.

Conflicts of Interest: The authors declare no conflict of interest.

Appendix A

From Equation (21) it follows that $\lg c_{H_3O^+} = \frac{(E-const)2F}{2.3RT}$ or $\ln c_{H_3O^+} = \frac{(E-const)2F}{RT}$. Then, $c_{H_3O^+} = \exp(\frac{(E-const)2F}{RT})$ and $\frac{dc_{H_3O^+}}{dt} = \exp(\frac{(E-const)2F}{RT}) \times \frac{2F}{RT}\frac{dE}{dt}$. If $i = nF \times dc/dt$, then $\lg i = \lg(nF) + \lg(dc/dt)$, $\lg(dc/dt) = \exp(\frac{(E-const)2F}{2.3RT})$ and $\lg i = const + \exp(\frac{(E-const)2F}{RT})$ or $d(\lg i) = \frac{2F}{2.3RT}dE$, which yields $\frac{dE}{d\lg i} = \frac{2.3RT}{2F} \approx 30$ mV/dec (derivation as for Equation (17) with cumulative constant term *const*).

References

1. Juodkazis, K.; Juodkazytė, J.; Jelmakas, E.; Kalinauskas, P.; Valsiūnas, I.; Mečinskas, P.; Juodkazis, S. Photoelectrolysis of Water: Solar Hydrogen-Achievements and Perspectives. *Opt. Express Energy Express* **2010**, *18*, A147–A160. [CrossRef]
2. Conway, B.E.; Tilak, B.V. Interfacial processes involving electrocatalytic evolution and oxidation of H_2, and the role of chemisorbed H. *Electrochim. Acta* **2002**, *47*, 3571–3594. [CrossRef]
3. Dubouis, N.; Grimaud, A. The hydrogen evolution reaction: From material to interfacial descriptors. *Chem. Sci.* **2019**, *10*, 9165–9181. [CrossRef] [PubMed]
4. Lasia, A. *Handbook of Fuel Cells*; John Wiley & Son, Ltd.: Hoboken, NJ, USA, 2010.
5. Lasia, A. On the mechanism of the hydrogen absorption reaction. *J. Electroanal. Chem.* **2006**, *593*, 159–166. [CrossRef]
6. Losiewicz, B.; Jurczakowski, R.; Lasia, A. Kinetics of hydrogen underpotential deposition at polycrystalline platinum in acidic solutions. *Electroch. Acta* **2012**, *80*, 292–301. [CrossRef]
7. Elayappana, V.; Shanmugamb, R.; Chinnusamyc, S.; Yoob, D.J.; Mayakrishnane, G.; Kima, K.; Noha, H.S.; Kima, M.K.; Lee, H. Three-dimensional bimetal TMO supported carbon based electrocatalyst developed via dry synthesis for hydrogen and oxygen evolution. *Appl. Surf. Sci.* **2020**, *505*, 144642. [CrossRef]
8. Logeshwaran, N.; Ramakrishnan, S.; Chandrasekaran, S.S.; Vinothkannan, M.; Kim, A.R.; Sengodan, S.; Velusamy, D.B.; Varadhan, P.; He, J.H.; Yoo, D.J. An efficient and durable trifunctional electrocatalyst for zinc–air batteries driven overall water splitting. *Appl. Catal. B Environ.* **2021**, *297*, 120405. [CrossRef]
9. Sui, Y.; Ji, X. Anticatalytic Strategies to Suppress Water Electrolysis in Aqueous Batteries. *Chem. Rev.* **2021**, *121*, 6654–6695. [CrossRef] [PubMed]
10. Vetter, K.J. *Elektrochemische Kinetik*; Springer: Berlin, Germany, 1961.
11. Will, F.G.; Knorr, C.A. Untersuchung von Adsorptionserscheinungen an Rhodium, Iridium, Palladium und Gold mit der potentiostatischen Dreieckmethode. *Z. Electrochem.* **1960**, *64*, 270–275.
12. Biegler, T.; Rand, D.A.J.; Woods, R. Limiting oxygen coverage on platinized platinum; Relevance to determination of real platinum area by hydrogen adsorption. *J. Electroanal. Chem.* **1971**, *29*, 269–277. [CrossRef]
13. Gomez, R.; Orts, J.M.; Alvarez-Ruiz, B.; Feliu, J.M. Effect of Temperature on Hydrogen Adsorption on Pt(111), Pt(110), and Pt(100) Electrodes in 0.1 M $HClO_4$. *J. Phys. Chem. B* **2004**, *108*, 228–238. [CrossRef]
14. Sudhagar, P.; Roy, N.; Vedarajan, R.; Devadoss, A.; Terashima, C.; Nakata, K.; Fujishima, A. *Photoelectrochemical Solar Fuel Production From Basic Principles to Advanced Devicess*; Springer: Berlin/Heidelberg, Germany, 2016.
15. Pourbaix, M. *Atlas D'équilibres Électrochimiques*; Gauthier-Villars: Paris, France, 1963.
16. Jerkiewicz, G. Standard and Reversible Hydrogen Electrodes: Theory, Design, Operation and Applications. *ACS Catal.* **2020**, *10*, 8409–8417. [CrossRef]
17. Juodkazis, K.; Juodkazytė, J.; Grigucevičienė, A.; Juodkazis, S. Hydrogen species within the metals: Role of molecular hydrogen ion H_2^+. *Appl. Surf. Sci.* **2011**, *258*, 743–747. [CrossRef]
18. Kriek, R.J.; Mogwase, B.M.S.; Vorster, S. Relation of the electrochemical interplay between H_2PtCl_6 and $H_2O/H_3O^+/H_2{}^+$ and the hydrogen-evolution reaction. *Electrochem. Sci. Adv.* **2021**, e2100041. [CrossRef]
19. Wang, Y.; Liu, Z.; Liu, H.; Suen, N.T.; Yu, X.; Feng, L. Electrochemical Hydrogen Evolution Reaction Efficiently Catalyzed by Ru 2 P Nanoparticles. *ChemSusChem* **2018**, *11*, 2724–2729. [CrossRef] [PubMed]
20. Sarkar, S.; Peter, S.C. An overview on Pd-based electrocatalysts for the hydrogen evolution reaction. *Inorg. Chem. Front.* **2018**, *5*, 2060–2080. [CrossRef]
21. Fan, X.; Du, P.; Ma, X.; Wang, R.; Ma, J.; Wang, Y.; Fan, D.; Long, Y.; Deng, B.; Huang, K.; et al. Mechanochemical Synthesis of Pt/Nb_2CT_x MXene Composites for Enhanced Electrocatalytic Hydrogen Evolution. *Materials* **2021**, *14*, 2426. [CrossRef]
22. Emsley, J. *The Elements*, 2nd ed.; Clarendon Press: Oxford, UK, 1991.
23. Markovic, M.M.; Ross, P.N., Jr. Surface science studies of model fuel cell electrocatalysts. *Surf. Sci. Rep.* **2002**, *45*, 117–229. [CrossRef]
24. Nobuhara, K.; Nakanishi, H.; Kasai, H.; Okiji, A. Interactions of atomic hydrogen with Cu(111), Pt(111), and Pd(111) . *J. Appl. Phys.* **2000**, *88*, 6897–6901. [CrossRef]
25. Jerkiewicz, G. Hydrogen sorption AT/IN electrodes. *Prog. Surf. Sci.* **1998**, *57*, 137–186. [CrossRef]

26. Jerkiewicz, G.; Zolfaghari, A. Comparison of Hydrogen Electroadsorption from the Electrolyte with Hydrogen Adsorption from the Gas Phase. *J. Electrochem. Soc.* **1996**, *143*, 1240–1248. [CrossRef]
27. Ooka, H.; Wintzer, M.E.; Nakamura, R. Non-Zero Binding Enhances Kinetics of Catalysis: Machine Learning Analysis on the Experimental Hydrogen Binding Energy of Platinum. *ACS Catal.* **2021**, *11*, 6298–6303. [CrossRef]
28. Yan, L.; Sun, Y.; Yamamoto, Y.; Kasamatsu, S.; Hamada, I.; Sugino, O. Hydrogen adsorption on Pt(111) revisited from random phase approximation. *J. Chem. Phys.* **2018**, *149*, 164702. [CrossRef] [PubMed]
29. Nordholm, S.; Bacskay, G.B. The Basics of Covalent Bonding in Terms of Energy and Dynamics. *Molecules* **2020**, *25*, 2667. [CrossRef]
30. Lopez, G.V.; Fournier, M.; Jankunas, J.; Spiliotis, A.K.; Rakitzis, T.P.; Chandler, D.W. Alignment of the hydrogen molecule under intense laser fields. *J. Chem. Phys.* **2017**, *147*, 013948. [CrossRef]
31. Armstrong, D.A.; Huie, R.E.; Koppenol, W.H.; Lymar, S.V.; Merényi, G.; Neta, P.; Ruscic, B.; Stanbury, D.M.; Steenken, S.; Wardman, P. Standard electrode potentials involving radicals in aqueous solution: Inorganic radicals (IUPAC Technical Report). *Pure Appl. Chem.* **2015**, *87*, 1139–1150. [CrossRef]
32. Huber, K.P.; Herzberg, G. *Molecular Spectra and Molecular Structure IV. Constants of Diatomic Molecules*; Springer: Boston, MA, USA, 1979.
33. Pavičić, D.; Kiess, A.; Hänsch, T.W.; Figger, H. Intense-Laser-Field Ionization of the Hydrogen Molecular Ions H_2^+ and D_2^+ at Critical Internuclear Distances. *Phys. Rev. Lett.* **2005**, *94*, 163002. [CrossRef] [PubMed]
34. Xu, H.; Li, Z.; He, F.; Wang, X.; Atia-Tul-Noor, A.; Kielpinski, D.; Sang, R.T.; Litvinyuk, I.V. Observing electron localization in a dissociating $H_2{}^+$ molecule in real time. *Nat. Commun.* **2017**, *8*, 15849. [CrossRef]
35. Sun, Z.; Yao, H.; Ren, X.; Liu, Y.; Wang, D.; Zhao, W.; Wang, C.; Yang, C. Imaging of electron transition and bond breaking in the photodissociation of H_2^+ via ultrafast X-ray photoelectron diffraction. *Opt. Express* **2021**, *29*, 10893–10902. [CrossRef]
36. Palascak, M.W.; Shields, G.C. Accurate Experimental Values for the Free Energies of Hydration of H^+, OH^-, and H_3O^+. *J. Phys. Chem. A* **2004**, *108*, 3692–3694. [CrossRef]
37. Juodkazis, K.; Juodkazytė, J.; Šebeka, B.; Juodkazis, S. Reversible hydrogen evolution and oxidation on Pt electrode mediated by molecular ion. *Appl. Surf. Sci.* **2014**, *290*, 13–17. [CrossRef]
38. Rabinovich, V.A.; Khavin, Z.Y. *Kratkiy Khimicheskiy Spravochnik*; Khimiya: Leningrad, Russia, 1977.
39. Jerkiewicz, G.; Vatankhan, G.; Lessard, J.; Soriaga, M.P.; Park, Y.S. Surface-oxide growth at platinum electrodes in aqueous H_2SO_4: Reexamination of its mechanism through combined cyclic-voltammetry, electrochemical quartz-crystal nanobalance, and Auger electron spectroscopy measurements. *Electroch. Acta* **2004**, *49*, 1451–1459. [CrossRef]
40. Juodkazytė, J.; Juodkazis, K.; Matulaitienė, I.; Šebeka, B.; Savickaja, I.; Balčytis, A.; Nishijima, Y.; Niaura, G.; Juodkazis, S. Hydrogen Evolution on Nano-Structured CuO/Pd Electrode: Raman Scattering Study. *Appl. Sci.* **2019**, *9*, 5301. [CrossRef]
41. Tafel, J. Über die Polarisation bei kathodischer Wasserstoffentwicklung. *Z. Für Phys. Chem.* **1905**, *50U*, 641–712
42. Butler, J.A.V. Studies in heterogeneous equilibria. Part II. The kinetic interpretation of the Nernst theory of electromotive force. *Trans. Faraday Soc.* **1924**, *19*, 729–733. [CrossRef]
43. Erdey-Gruz, T.; Volmer, M. Zur theorie der wasserstoffüberspannung. *Z. Phys. Chem.* **1930**, *150*, 203–213. [CrossRef]
44. Bazant, M.Z. Theory of Chemical Kinetics and Charge Transfer based on Nonequilibrium Thermodynamics. *Acc. Chem. Res.* **2013**, *46*, 1144–1160. [CrossRef] [PubMed]
45. Chen, M.; Santra, L.Z.B.; Ko, H.Y.; Di Stasio, R.A.; Klein, M.L.; Car, R.; Wu, X. Hydroxide diffuses slower than hydronium in water because its solvated structure inhibits correlated proton transfer. *Nat. Chem.* **2018**, *10*, 413–419. [CrossRef] [PubMed]
46. Li, Y.; Jiang, K.; Yang, J.; Zheng, Y.; Hübner, R.; Ou, Z.; Dong, X.; He, L.; Wang, H.; Li, J.; et al. Tungsten Oxide/Reduced Graphene Oxide Aerogel with Low-Content Platinum as High-Performance Electrocatalyst for Hydrogen Evolution Reaction. *Small* **2021**, *17*, 2102159. [CrossRef]
47. Takenaka, M.; Hashimoto, Y.; Iwasa, T.; Taketsugu, T.; Seniutinas, G.; Balcytis, A.; Juodkazis, S.; Nishijima, Y. First Principles Calculations Toward Understanding SERS of 2,2′-Bipyridyl Adsorbed on Au, Ag, and Au–Ag Nanoalloy. *J. Comput. Chem.* **2004**, *40*, 925–932. [CrossRef] [PubMed]
48. Kronberg, R.; Laasonen, K. Reconciling the Experimental and Computational Hydrogen Evolution Activities of Pt(111) through DFT-Based Constrained MD Simulations. *ACS Catal.* **2021**, *11*, 8062–8078. [CrossRef]
49. Lindgren, P.; Kastlunger, G.; Peterson, A.A. A Challenge to the $G \sim 0$ Interpretation of Hydrogen Evolution. *ACS Catal.* **2020**, *10*, 121–128. [CrossRef]
50. Nishijima, Y.; Shimizu, S.; Kurihara, K.; Hashimoto, Y.; Takahashi, H.; Balcytis, A.; Seniutinas, G.; Okazaki, S.; Juodkazyte, J.; Iwasa, T.; et al. Optical readout of hydrogen storage in films of Au and Pd. *Opt. Express* **2017**, *20*, 24081–24092. [CrossRef] [PubMed]